

Numerical study of turbulent forced convection nanofluid jet flow in a converging sinusoidal channel

A. Taheri ¹; E. Aboukazempour ²; A. Ramiar ³; A. A. Ranjbar ³; M. Rahimi-Esbo ^{*,3}

¹School of Mechanical Engineering, Mazandaran University of Science and Technology, Babol, Iran

²Department of Mechanical Engineering, Iran University of Science and Technology, Narmak, Tehran, Iran

³School of Mechanical Engineering, Babol University of Technology, P. O. Box 484, Babol, Iran

Received 10 March 2015; revised 26 July 2015; accepted 10 October 2015; available online 04 December 2015


ABSTRACT: Research in convective heat transfer using suspensions of nanometer-sized solid particles in base liquids started only over the past decade. Recent investigations on nanofluid, suspensions are often called, show that the suspended nanoparticles remarkably change the transport properties and heat transfer characteristics of the suspension. Bending walls can also improve heat transfer by raising the total heat transfer from a surface and changing the behavior of the flow. In this paper two-dimensional incompressible nanofluid flow in a confined sinusoidal converging jet in turbulent flow regime is numerically investigated. Results showed for the flow structure at different Reynolds numbers for steady asymmetric jet development at various values of the duct-to-jet width ratio (aspect ratio), different amplitudes of surface undulation and different volume fractions of nanoparticles. For considering unsteady treatment of the flow, the streamlines and temperature contours result for the unsteady problem is presented and compared with the steady results. The present computations are in a good agreement with experimental results in open literature. The results show that by increasing the Reynolds number, aspect ratio, amplitude and volume fraction the average the Nusselt number will increase.

Keywords: Aspect ratio; Nanoparticles; Nusselt number; Recirculation region; Wavy wall.

INTRODUCTION

Convective heat transfer can be enhanced passively by changing the flow geometry, the boundary conditions, or by enhancing the thermal conductivity of the fluid. Various techniques have been proposed to enhance the heat transfer properties of fluids. Changing geometry, by raising heat transfer surface the behavior of the flow will increase the total heat transfer. Using porous media, micro scale channels, increasing the surface and placing a shackle in the way of the fluid are common ways of increasing heat transfer by changing the geometry. Researchers have also tried to raise the thermal conductivity of base fluids by suspending micro- or larger-sized solid particles in fluids, since the thermal conductivity of a solid is typically higher than that of liquids. However, due to the large size and high density of the particles, there is

not adequate way to prevent the solid particles from settling out of suspension. The lack of stability of such suspensions induces added flow resistance and possible erosion. Therefore, fluids with dispersed coarse-grained particles have not yet been commercialized. Modern nanotechnology provides new opportunities to process and produce materials with average crystallite sizes below 50 nm. Fluids with suspended nanoparticles are called nanofluid, a term proposed by Choi [1] of the Argonne National Laboratory, USA nanofluids can be considered to be the next generation heat transfer fluids because they offer exciting new possibilities to enhance the heat transfer performance compared to pure liquids. They are expected to have superior properties compared to conventional heat transfer fluids, as well as fluids containing micro-sized metallic particles. The much larger relative surface area of nanoparticles, compared to those of conventional particles, should not only significantly improve heat transfer capabilities, but also

 *Corresponding Author: Mazaher Rahimi-Esbo
Email: rahimi.mazaher@gmail.com
Tel.: (+98) 98911 6277073
Fax: (+98) 98911 6277073

should raise the stability of the suspensions. Also, nanofluid can improve abrasion-related properties as compared to the conventional solid/fluid mixtures. To explain the reasons for the anomalous increase of the thermal conductivity in nanofluid, Koblinski *et al.* [2] and Eastman *et al.* [3] proposed four possible mechanisms, e.g., Brownian motion of the nanoparticles, molecular-level layering of the liquid at the liquid/particle interface, the nature of heat transport in the nanoparticles, and the effects of nanoparticles clustering.

Many researchers applied nanofluid in different applications. Zhang *et al.* [4] numerically investigated heat transfer enhancement of Al_2O_3 -water nanofluids in natural convection in heated wavy cavities. They studied the effects of Rayleigh number, amplitude of wavy wall and volume fraction of nanofluids on the flow field and temperature distribution. They reported that the effects of this parameter are more effective on the flow field than on temperature distribution. A set of experimental data and some correlation for nanofluid properties are available in the paper of Ravikanth *et al.* [5] for a fully developed turbulent regime. Primary fluid was a mixture of 60% ethylene glycol and 40% water by mass. Aluminum oxide, copper oxide and silicon dioxide were used as nanoparticles. An 80% enhancement has been seen with a 10% volumetric fraction aluminum oxide. However a fourfold increase of pressure drop happens for this nanofluid. Sundar and Sharma [6] reported a 30% enhancement in heat transfer caused by adding nanoparticles. They used aluminum oxide as nanoparticles and performed their experiments for Reynolds number range of 10000-22000. They also defined equations for Nusselt number and friction coefficient for nanofluid in turbulent flow regime. Another set of experimental data for nanoparticles is reported by Duangthongsuk and Wongwises [7] for a water based fluid containing 0.2 % volume fraction of TiO_2 . With 21nm diameter nanoparticles were used in their research. Results showed that convective heat transfer coefficient of nanofluid is about 6-11 % greater than the base fluid. Meanwhile adding nanoparticles has a little penalty on the pressure drop. However Fotukian and Esfahany [8] did not see a remarkable enhancement in heat transfer due to adding nanoparticles. Their experiments were much like to the Duangthongsuk and Wongwises [7] work except with the nanoparticles which was Al_2O_3 . Their measurement showed that pressure drop for dilute nanofluid than that of base flow. Ghaffari *et al.* [9]

numerically investigated turbulent mixed convection heat transfer of a nanofluid consisting of water and Al_2O_3 through a horizontal curved tube. They carried out two-phase mixture model to study such a flow field. They reported that the nanoparticle volume fraction does not have a direct effect on the secondary flow and the skin friction coefficient; however, its effects on the thermal parameters and flow turbulence intensity are significant.

Also many works are recorded at the field of wavy channel and converging channel. Nishimura and Matsune [10] numerically investigated pulsated flow for low Reynolds number in a wavy wall channel. They compared their numerically generated results with visualized flow behavior that they presented in their work. They have reported that time-average vortex strength and wall shear stresses first increase, as frequency of the oscillation raises under a fixed mass flow rate and then, for above a certain value of frequency decreases because of viscous effects. Tolentino *et al.* [11] presented experimental flow visualization for a converging channel with wavy walls. They studied the flow behavior for different Reynolds numbers and converging/diverging angles. They found that a diverging channel has a better effect in a chaotic mixture as flow is more stable for a converging channel even with a higher Reynolds number. Another simulation of turbulent flow in wavy channel was performed by Habib *et al.* [12] for a wide range of Reynolds numbers. Their research shows good agreement with the experimental data. They found that the local Nusselt number takes its greatest value in the peak of waves where the velocity of the fluid is maximum. However friction coefficient also shows the same behavior. They reported enhancement of heat transfer due to bending walls, especially for greater amplitude to wavelength ratios. Also Pham *et al.* [13] employed large-eddy simulation to address a major point in heat transfer by studying fluid flow behavior in sinusoidal wavy channels for a wide range of Reynolds number levels. They investigated the effect of spacing ratio, waviness parameter, Reynolds and Prandtl number on flow structure and Nusselt number. Zhang *et al.* [14] compared their numerical predictions of the f (Fanning friction factor) and j (Colburn factor) with experimental investigations in the range of $10 \leq \text{Re} \leq 1500$ and according to the authors, the numerical and experimental data are in excellent agreement. In their study, numerical simulations were carried out for

two sinusoidal geometries in the given Reynolds number range while experimental tests were performed for similar geometries in a wider Reynolds range (Re 7000).

Furthermore, there are papers in the literature in the turbulence modeling in backward facing step and converging channel. For examples Yang *et al.* [15] presented a numerical study of homogeneous turbulent shear flow and turbulent flow past a backward-facing step using different linear and non-linear turbulence models. Driver *et al.* [16] experimentally investigated turbulent flow past a backward-facing step. In their experiment the ratio of step height to the tunnel exit was 9. Shariati *et al.* [17] investigated the flow through the converging zone of a headbox, numerically and experimentally. The experimental headbox that was used is a laboratory scale model of a typical headbox with the size reduced by a factor of 5. The main focus of their study was on the turbulence quantities and secondary flows in the outlet jet. They reported the turbulence kinetic energy computed numerically is much higher than that measured experimentally. Zhang [18] measured the fiber orientations along the centerline of an asymmetric headbox. He also predicted the fiber orientation in both symmetric and asymmetric headboxes using a fiber model, but only using the mean flow field got from the k “ model. His comparison between the measured and predicted results showed that the simulated orientations tend to align more with the flow than the experimentally observed results because the turbulence was not taken into consideration for his calculations. Feng *et al.* [19] carried out a large eddy simulation (LES) to model the flow field in a converging section. They used a Lagrangian tracking scheme to simulate the motion of flexible or rigid individual fibers.

There are also many works in the field of jet flow. Sarma *et al.* [20] investigated the 2D incompressible jet development inside a duct in the laminar flow regime for cases with and without entrainment of ambient fluid. However, they didn't solve the energy equation. The variation of critical Reynolds number for bifurcation with aspect ratio has been investigated in details by Battaglia *et al.* [21]. Al-Aswadi *et al.* [22] investigated laminar forced convection flow of different nanofluids over a 2D horizontal backward facing step placed in a duct. They reported that the reattachment point moves downstream far from the step as Reynolds number increases, and nanofluid containing SiO₂

nanoparticles has the highest velocity among the other nanofluid types, while nanofluid of Au nanoparticles has the lowest velocity.

Although some researchers have investigated nanofluids in turbulent flow, none of them investigated the turbulent nanofluid jet flow in a converging wavy channel. In this paper the contemporaneous effect of adding Al₂O₃ nanoparticles and jet flow on the improvement of heat transfer properties in a converging wavy channel is investigated. Also the effect of aspect ratios (duct width / jet width) and amplitude on flow features and heat transfer properties is investigated. Jet flows are encountered in a wide variety of applications, such as gas turbine combustors, industrial burners, ejector systems, rocket nozzles and the like. The aim of this study is to get an understanding of the velocity and temperature distribution, Nusselt number along top and bottom walls downstream from the jet and velocity profile at different sections. Moreover, the performance of the jet flow at various Reynolds numbers is investigated. Also the effect of nanoparticles on thermal and flow characteristics and the effect of aspect ratios on flow features and heat transfer properties are investigated. In this research Al₂O₃-H₂O is used. The thermal conductivity of Al₂O₃ which is used in this research is roughly one tenth of Cu; however, the unique property of Al₂O₃ is its low thermal diffusivity. The reduced value of thermal diffusivity leads to higher temperature gradients and therefore, more heat transfer enhancement

EXPERIMENTAL

Computational Methods

2D incompressible turbulent jet flow in a wavy converging channel is considered. For simplicity, the jet is taken as isothermal. The velocity profile at the jet inlet is taken as uniform. The geometry considered and the flow configurations used in this work are shown in Fig. 1. The nanoparticles and the base fluid (i.e. water) are assumed to be in thermal equilibrium and no slip condition occurs between them. The other boundary conditions are mentioned in Fig. 1.

Aspect ratio is taken as:

$$AR = h/d \quad (1)$$

The continuity, momentum and energy equations for the 2D flow problem are given by:

1. Continuity:

$$\frac{\partial}{\partial x_i} (\rho_{nf} u_i) = 0 \quad (2)$$

2. Momentum:

$$\frac{\partial}{\partial x_j} (\rho_{nf} u_i u_j) = -\partial p / \partial x_i + \frac{\partial}{\partial x_j} \left[\mu (\partial u_i / \partial x_j + \partial u_j / \partial x_i) \right] + \frac{\partial}{\partial x_j} (-\rho_{nf} \overline{u'_i u'_j}) \quad (3)$$

3. Energy:

$$\frac{\partial}{\partial x_i} (\rho_{nf} u_i T) = \frac{\partial}{\partial x_j} \left((\Gamma + \Gamma_t) \frac{\partial T}{\partial x_j} \right) \quad (4)$$

where Γ and Γ_t are the molecular thermal diffusivity and turbulent thermal diffusivity, respectively, and are given by:

$$\Gamma = \mu_{nf} / Pr_{nf}, \quad \Gamma_t = \mu_t / Pr_t \quad (5)$$

The Reynolds-averaged approach to turbulence modeling requires that the Reynolds stresses, i.e. $\overline{u'_i u'_j}$ needs to be modeled. For this purpose the $k - \epsilon$ model is chosen. A common method employs the Boussinesq hypothesis to relate the Reynolds stresses to the mean velocity gradients:

$$\rho_{nf} \overline{u'_i u'_j} = \mu_t (\partial u_i / \partial x_j + \partial u_j / \partial x_i) \quad (6)$$

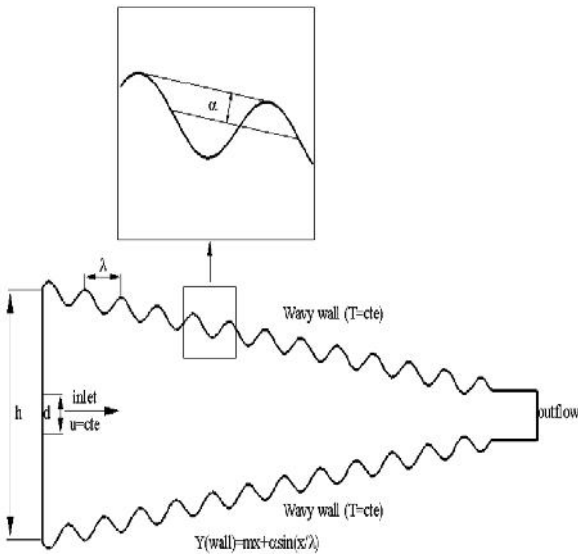


Fig. 1: Geometry and boundary condition of the problem

The turbulent viscosity term is to be computed. It is defined by the following equation:

$$\mu_t = \rho_{nf} C_\mu k^2 / \epsilon \quad (7)$$

4. Transport equation for k and ϵ

$$\frac{\partial}{\partial x_i} (\rho_{nf} k u_i) = \frac{\partial}{\partial x_j} \left[\left(\mu_{nf} + \frac{\mu_t}{\sigma_k} \right) \frac{\partial k}{\partial x_j} \right] + G_k - \rho_{nf} \epsilon + S_k \quad (8)$$

and

$$\frac{\partial}{\partial x_i} (\rho_{nf} \epsilon u_i) = \frac{\partial}{\partial x_j} \left[\left(\mu_{nf} + \frac{\mu_t}{\sigma_\epsilon} \right) \frac{\partial \epsilon}{\partial x_j} \right] + C_{1\epsilon} \frac{\epsilon}{k} G_k + C_{2\epsilon} \rho_{nf} \frac{\epsilon^2}{k} + S_\epsilon \quad (9)$$

where G_k is the rate of generation of the TKE and ϵ is its destruction rate, and is written as:

$$G_k = -\rho_{nf} \overline{u'_i u'_j} \frac{\partial u_j}{\partial x_i} \quad (10)$$

S_k, S_ϵ are source terms for k and ϵ in this research are taken as zero. The boundary values for the turbulent quantities near the wall are specified with the standard wall-treatment method. The values of $C_\mu = 0.009, C_1 = 1.44, C_2 = 1.92, \sigma_k = 1, \sigma_\epsilon = 1.3$ and $Pr_t = 0.9$ are chosen to be the empirical constants in the turbulent transport equations. It is showed by Launder and Spalding [23]. According to Rostamani *et al.* [24] suggestion the following equations are used to calculate the turbulent intensity (I), turbulent kinetic energy (k) and turbulent dissipation rate (ϵ) at the inlet section of the headbox.

$$\begin{aligned} I &= 0.16 \text{Re}^{-1/8} \\ k &= (3/2)(I \times u_{in})^2 \\ \epsilon &= c_\mu^{0.75} \times (k^{1.5} / 0.1h) \end{aligned} \quad (11)$$

Thermophysical properties of nanofluid

1. Thermal conductivity:

The thermal conductivity of the nanofluid is calculated from Chon *et al.* [25], which is expressed in the following form:

$$\frac{K_{nf}}{K_f} = 1 + 64.7 \phi^{0.746} (d_j / d_p)^{0.369} \times (K_p / K_f)^{0.7476} Pr_f^{0.9955} Re_p^{1.2521} \quad (12)$$

$$Pr_f = \mu_f / \rho_f \alpha_f \quad (13)$$

$$Re_p = \rho_f K_b T / 3 \pi \mu^2 l_f \quad (14)$$

$$d_p = 36 \times 10^{-9} \text{ m} \quad (15)$$

k_b is the Boltzmann constant, 1.3807×10^{-23} and l_f is the free average distance of water molecules that according to suggestion of Chon *et al.* is taken as 17 nm. Minista *et al.* [26] approved the accuracy of this model.

2. Viscosity:

The viscosity of the nanofluid is approximated as viscosity of the base fluid μ_f containing dilute suspension of fine spherical particles as given by Masoumi *et al.* [27].

$$\frac{\mu_{nf}}{\mu_f} = 1 + \rho_p V_b d_p^2 / 72 N \delta$$

$$N = (c_1 \phi + c_2) d_p + (c_3 \phi + c_4)$$
(11)

$$\delta = \sqrt[3]{\pi / 6 \phi} \times d_p$$

$$V_b = (1 / d_p) \sqrt{18 k_b T / \pi \rho_p d_p}$$

N is a parameter for adapting the results with experimental data where $c_1 = -1.133 \times 10^{-6}$, $c_2 = -2.771 \times 10^{-6}$, $c_3 = -9.0 \times 10^{-8}$ and $c_4 = -3.93 \times 10^{-7}$.

3. Density and specific heat:

The density and specific heat of the nanofluid are calculated by using the Pak and Cho [28] correlations, which are defined as:

$$\rho_{nf} = \phi \rho_p + (1 - \phi) \rho_f$$
(17)

$$(c_p)_{nf} = ((1 - \phi) \times \rho_f \times (c_p)_f + \phi \times (\rho \times c_p)_p) / \rho_{nf}$$
(18)

$$Pr_{nf} = \mu_{nf} \times c_{p_{nf}} / K_{nf}$$
(19)

The nondimensional flow and heat transfer parameters are defined by:

$$Re = 2 \rho_f U_{in} d / \mu_f$$
(20)

$$Nu = 1 \times (K_{nf} \partial T / \partial n) / (K_f (T_w - T_B))$$
(21)

Numerical procedure and code validation

A finite volume technique on a collocated grid is implemented for discretizing the governing equations inside the computational domain. The SIMPLE algorithm is used to link the pressure and velocity fields. For the stability of the solution, the diffusion term in the momentum equations is approximated by the second order central difference scheme. Moreover, a deferred correction scheme is adopted for the

convective terms. The second order upwind scheme is used for discretizing the convection term in turbulent equations. For the unsteady term implicit Euler method is applied. No quadrilateral elements and non-uniform grid systems are employed in the simulations. As depicted in Fig. 2 the grid is highly concentrated close to the jet to ensure the accuracy of the numerical simulations and for saving both the grid size and the computational time. At the end of any iteration, the residual sum for each of the conserved variables is computed and stored, thus recording the convergence history. The convergence criterion required that the maximum sum of the error for each of the conserved variables be smaller than 1×10^{-5} . Grid densities of 300×60 , 450×80 , 550×100 and 650×120 were selected to perform a grid independence test and they show less than a 1% difference in velocity compared to the chosen grid (550×100). This is shown in Fig. 3.

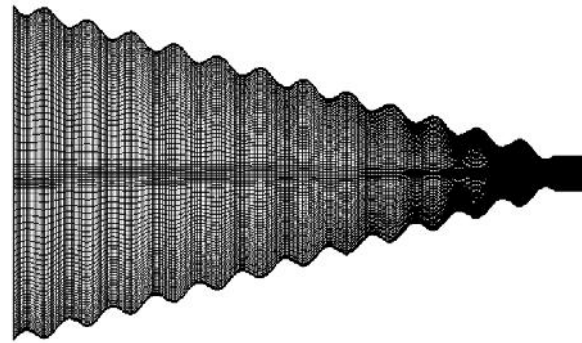


Fig. 2: Employed mesh geometry in the modeling

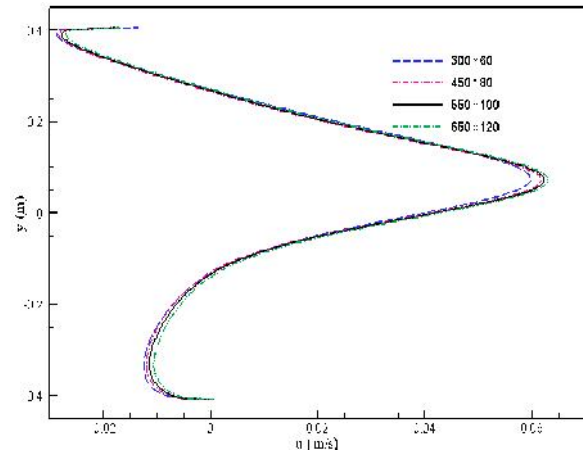


Fig. 3: velocity profile at x=0.5 for mesh independency investigation at Re=10000, AR=5 and w= 0%

As no work on nanofluid in a converging jet is recorded in literature for validating of the code two different cases are used. The present results are compared with the simulation of Zhang Xiaosi [18] and experimental data of Shariati *et al.* [17] in converging jet. As it can be seen from Fig. 4 (a) there is a very excellent agreement between results. Also for the case of sinusoidal channel the results are compared with experimental data of Zhang *et al.* [14] and numerical results of Pham *et al.* [13]. As it can be seen from Fig. 4 (b) there is an acceptable accuracy.

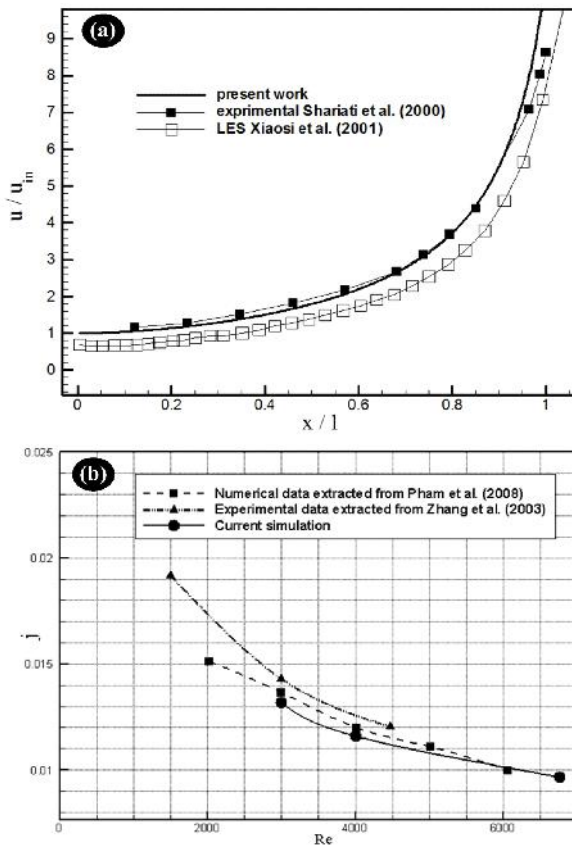


Fig. 4: (a) Velocity distributions at midline for a converging channel at $u_{in} = 1.22$ (m/s); (b) Global variations of j heat transfer coefficient versus Reynolds numbers for a wavy channel configuration

RESULTS AND DISCUSSION

Simulations are performed for different Reynolds numbers of 4000, 10000, 20000, 30000 and 40000, and various volume fraction of nanofluid 1%, 2%, 3%, 4% and 5% are compared to their pure base fluid (water)

furthermore, the simulations are carried out for different aspect ratios of 1, 2, 5, 10 and 20 and different amplitudes of 0.02, 0.03 and 0.04. The flow expands from uniform profile and separates to form a primary recirculation region at the upper and lower plate. After that, the velocity profile reattaches and redevelops approaching a fully developed flow as fluid flows toward the channel exit.

For the case of $AR=20$, $Re=15000$ unsteady solution is applied and the streamline and temperature contour simultaneous is depicted in Fig. 5. It is observed that after $t=400$ seconds the streamlines remain fixed. After this time, both steady and unsteady solutions have the same result and asymmetric flow occurs for both cases. It should be noted that the asymmetry in the flow pattern corresponds to a bimodal steady configuration with the jet turning upwards or downwards in a random way, during any computational run. Sarma *et al.* [20] presented this behavior in their papers. According to the above proof, the steady solution can be generalized to the unsteady problem. From now on results are reported for the steady state condition.

In Fig. 6 the steady state streamline patterns at different aspect ratios are depicted. In this figure the influence of aspect ratio on flow structure at $Re=15000$ and $w_1 = 0\%$ is shown. It is observed that for a low aspect ratio such as $AR=2$, the jet develops almost symmetrically and counter-rotating velocities are seen immediately after the sudden expansion. The jet decay is rapid and transition from jet-to-duct flow occurs in a short distance. At a higher aspect ratio of $AR=20$, it is observed that the steady state jet flow development is asymmetric. the transition from jet-to-duct flow occurs over a longer distance as well.

In Fig. 7, the influence of amplitude on flow structure at $Re=15000$ and $w_1 = 0\%$ is shown. It is observed that for low amplitude there isn't any recirculation zone in the dip of the wall. At higher amplitude of $a = 0.04$, it is observed that a recirculation zone forms in any dip of the sinusoidal wall. These zones have a great effect on increasing the local Nusselt number. Fig. 8 shows the distribution of the Nusselt number at the lower wall for $Re = 10000$ using different nanoparticles volume fractions. The figure illustrates an enhancement in Nusselt number by increasing the volume fraction of nanoparticles. This behavior can be inferred from Eq. (21). The effect of nanoparticles on the temperature difference term is negligible.

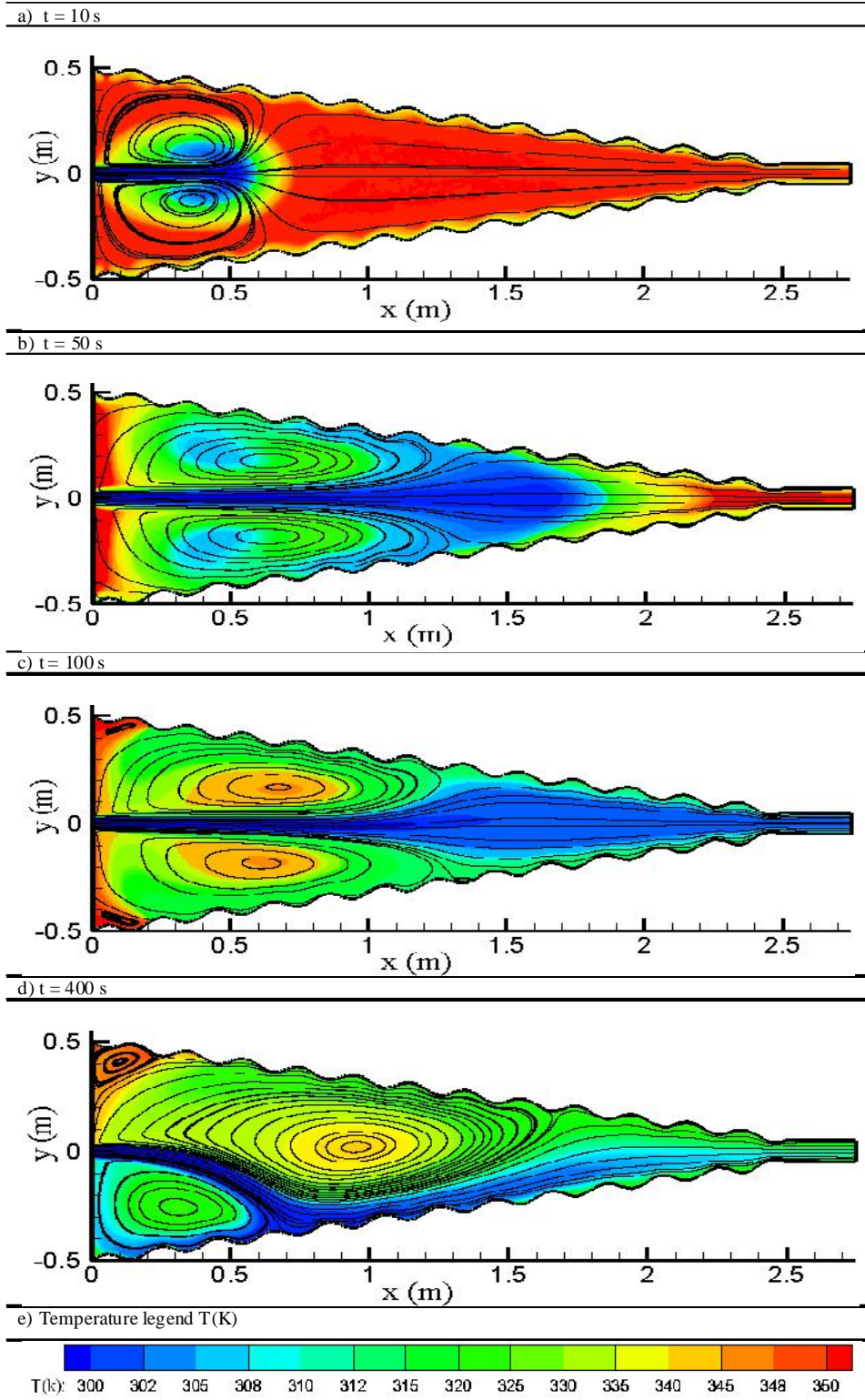


Fig. 5: Streamline contours for unsteady solution at $AR=20$, $Re=15000$ and $\Gamma = 0.02$

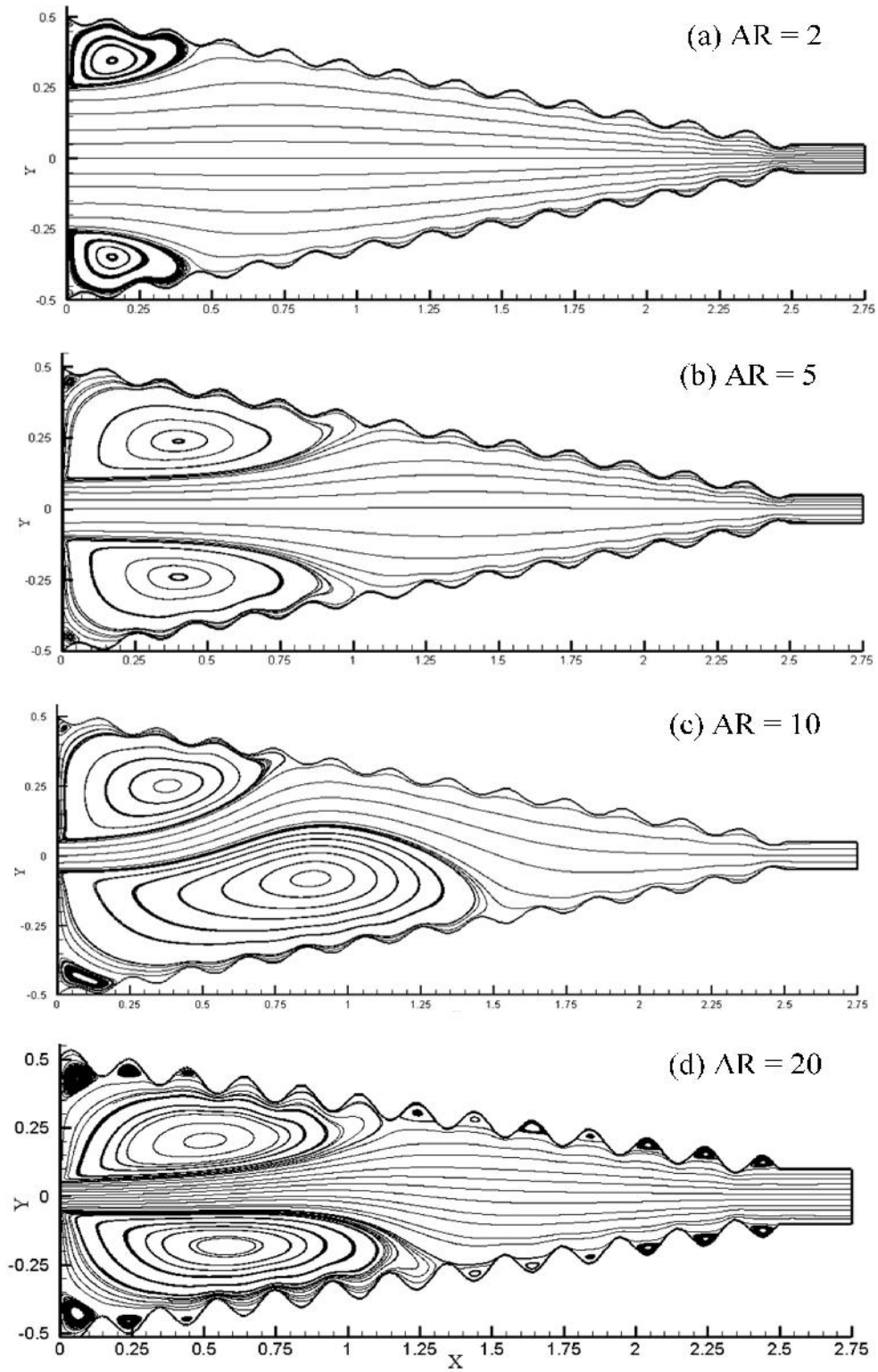


Fig. 6: Streamline contours for different aspect ratio at $Re=15000$, $wI=0\%$

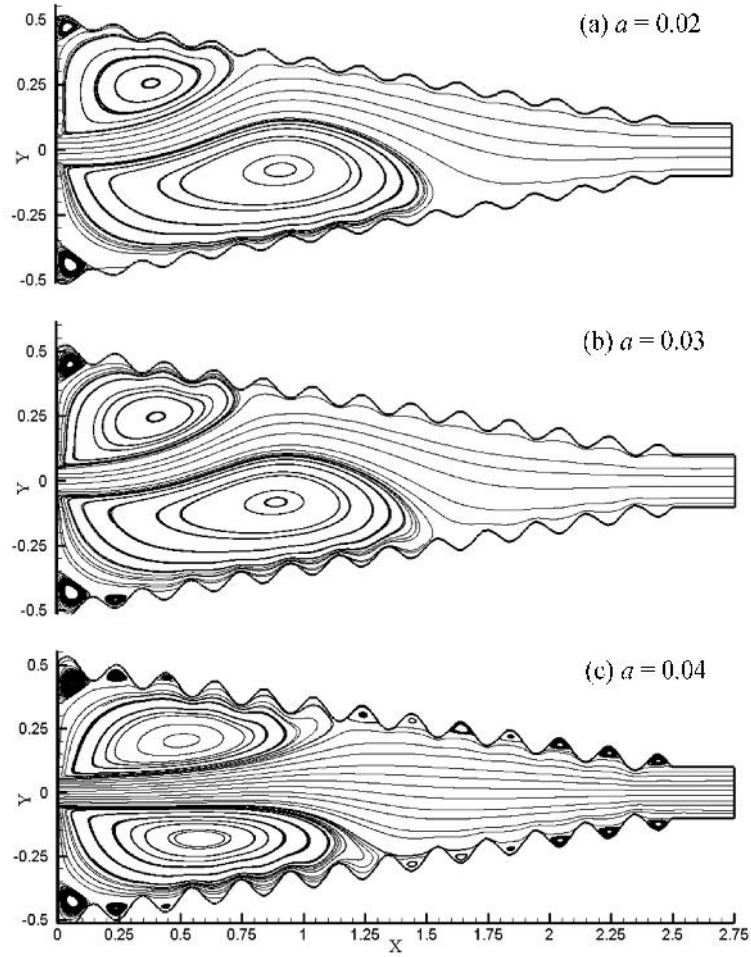


Fig. 7: Streamline contours for different amplitude at $Re=10000$, $wl= 0\%$

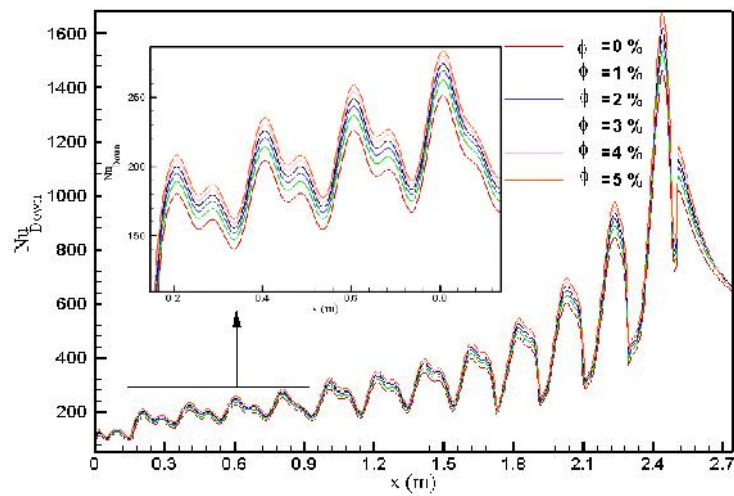


Fig. 8: Effect of volume fraction of nanoparticles (w) on Nusselt number at $Re=10000$ and $AR=5$

Effects of volume fraction of nanoparticles on the temperature gradient term and on the thermal conductivity ratio term are more pronounced. Before the point of reattachment as the volume fraction percentage of nanoparticles intensifies the temperature gradient at the top wall raises. This is related to the addition inertia forces as depicted by Eq. (3). The equations show that any increase in volume fraction raises inertia forces because \dots_{nf} will be increased and accordingly increases the temperature gradient. Besides, the nanoparticles increase the thermal conductivity ratio term as it can be seen from Eq. (12). So the temperature gradient term and thermal conductivity ratio term rise by increasing the volume fraction of nanoparticles. Therefore, it can be seen that by increasing volume fraction the Nusselt number will be increased, because the heat transfer properties is improved. Two sudden growths is sawn arrangement at the position of vortex zone.

The present computations show that when the volume fraction increases gradually from 0.0 to 0.03 and 0.05 the averaged Nusselt numbers will be raise from 369.96 to 407.183 and 422.223, respectively. As mentioned above, nanoparticles improve therrmophysycal properties of the fluid. They directly increase the Nusselt number.

The effect of aspect ratio on Nusselt number is depicted in Fig. 9. As aspect ratio increases the influences of the jet and recirculation zones are increased. Also chaotic behavior of the fluid flow will be increased and will have more of an impact between molecules of the fluid and the walls. These impacts lead to more energy absorption by the fluid .This leads to an average Nusselt number increase on both top and bottom walls.

The effect of amplitude of wall undulation on Nusselt number is depicted in Fig. 10. By increasing amplitude recirculation zones are formed in the dips of the wall. Chaotic behavior of the fluid flow will be raised and will have more impact between molecules of the fluid and the walls. These impacts cause more energy absorption by the fluid .These cause an average Nusselt number increase on top and bottom walls.

When, amplitude of the wavy wall is 0.0, 0.01, 0.02, 0.03, and 0.04, the averaged Nusselt number on bottom wall will gain the value of 321.711, 329.82, 361.439 and 392.727, respectively. These result are got at $Re=15000$ and $wl= 0\%$. High amplitude enhance heat transfer surface and changing the behavior of the flow regime enhance the total heat transfer. In any dip of the wall a circulation zone is formed that has a great impact on increasing the local Nusselt number.

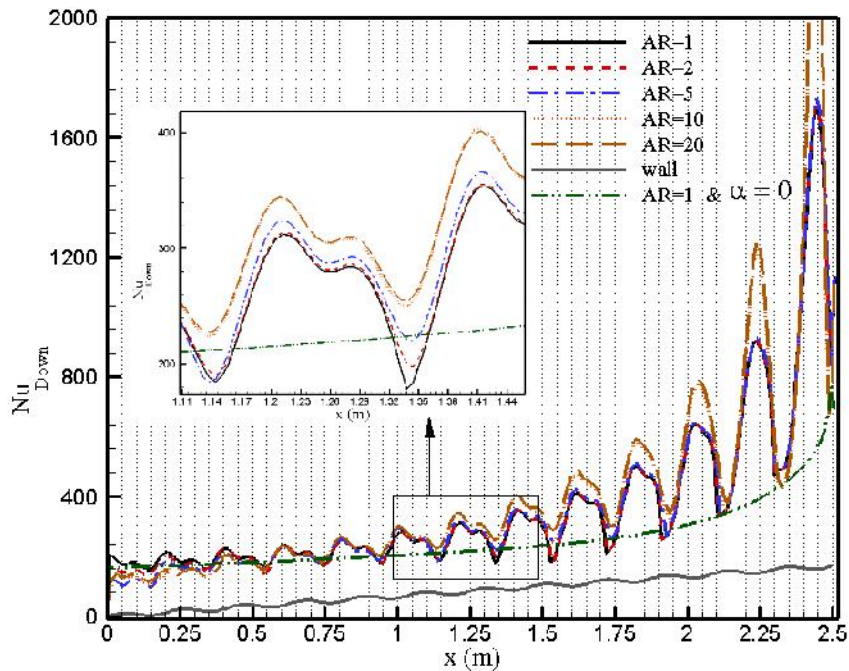


Fig. 9: Effect of aspect ratio on Nusselt number at $Re=15000$ and $wl= 0\%$

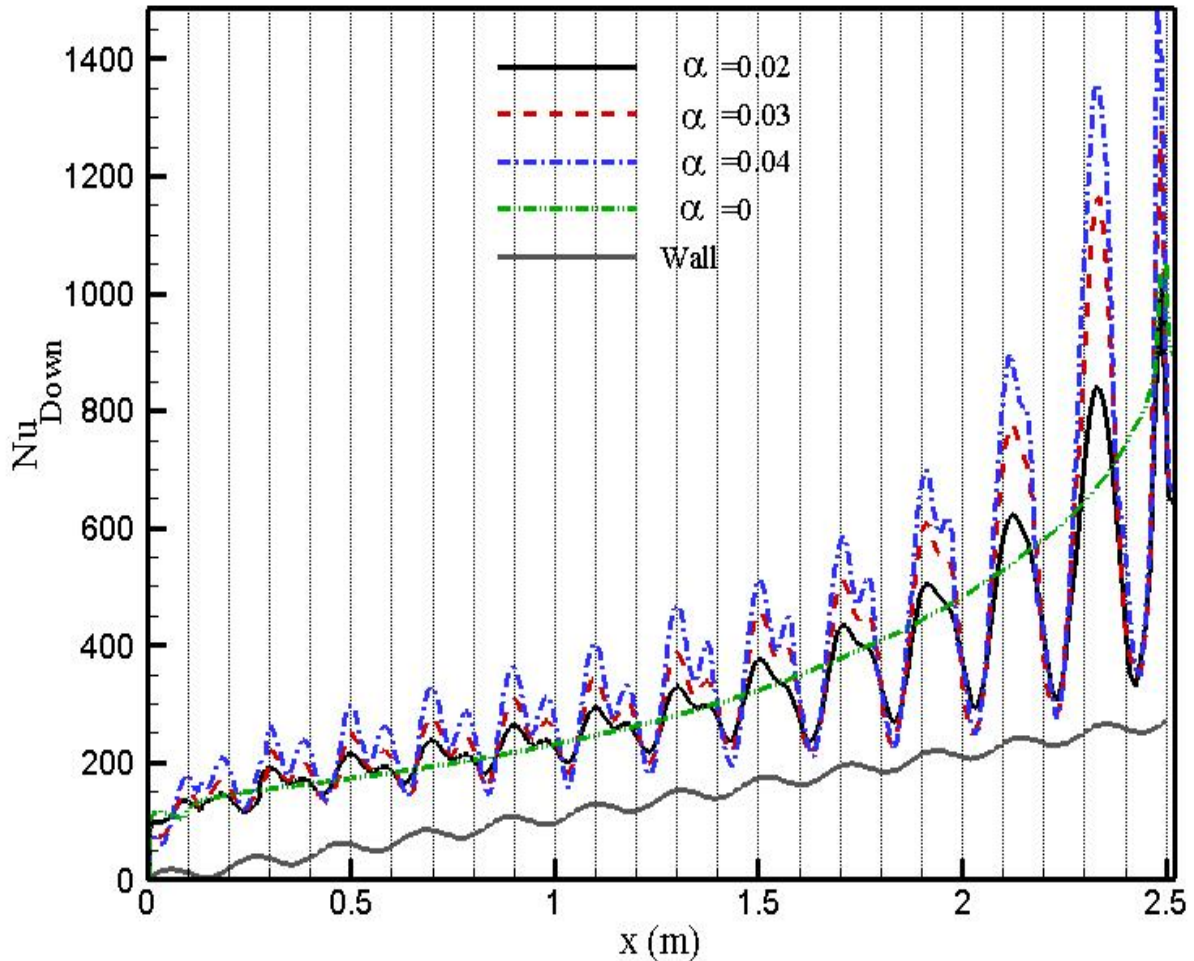


Fig. 10: Effect of amplitude on Nusselt number at $Re=10000$ and $wl=0\%$

Fig. 11 shows the particle volume concentration and flow Reynolds number effects on the average Nusselt number. It can be seen that the average Nusselt number increases with a rise in the nanoparticle volume concentration as well as an increase in the flow Reynolds number. This behavior is expected since the higher nanoparticle concentration increases the thermal conductivity of the nanofluid and higher Reynolds numbers raise the length of the recirculation zones thus causing an increase in the heat transfer rate.

Also, the figure shows that the average Nusselt number is more sensitive to volume fraction than to Reynolds number. For example at $Re=40000$ increasing volume fraction of 0 % to 5 % is caused 13.63 %

enhancement on average Nusselt number and at volume fraction of 5 % increasing Reynolds number 4000 to 20000 is caused more than 80 % enhancement.

The pressure drops at different amplitudes of wall undulations and volume fractions are depicted in Fig. 12. An increase in pressure drop is detected by raising the amplitude and volume fraction. In the Fig. 12a different amplitudes have been considered and the ratio of inlet width to the outlet width was 2.5. On the other hand, in Fig. 12b different volume fractions have been considered and the ratio of inlet width to the outlet width was 5. It can be seen that these parameters have negligible effect on the pressure drop. So, increasing in the pressure drop is negligible compared to heat transfer enhancement.

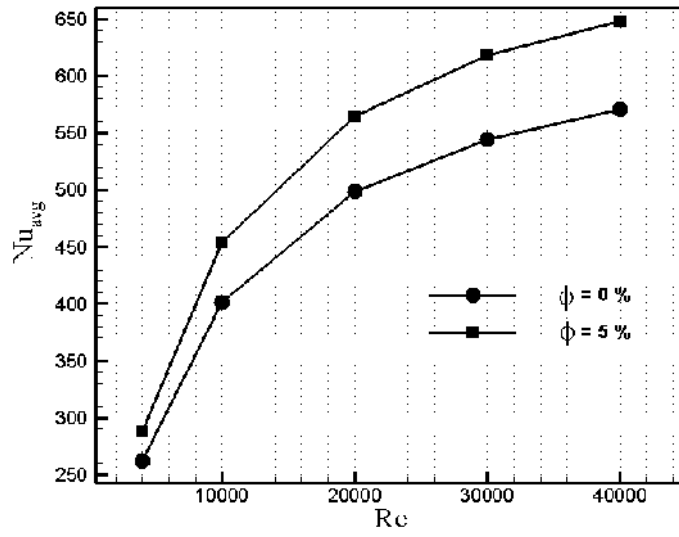


Fig. 11: The effect of nanoparticles volume fraction and Reynolds number on averaged Nusselt number at AR=10.

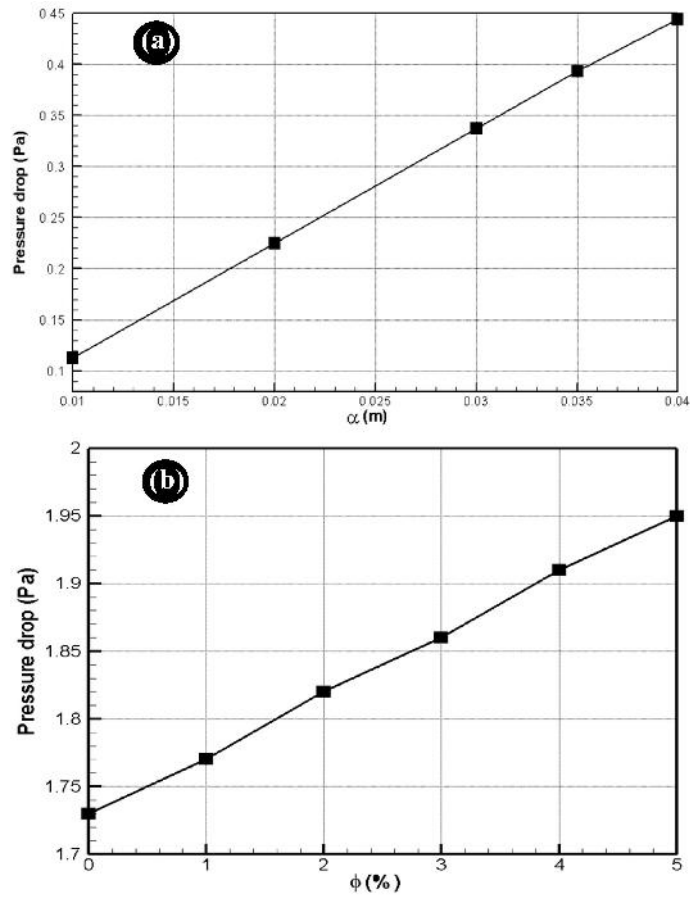


Fig. 12: (a) Pressure drop for different amplitude at $Re=10000, |w|=0\%$; (b) Pressure drop for different amplitude at $Re=10000, AR=5$

CONCLUSION

Forced convection of a turbulent nanofluid flow in a converging sinusoidal channel numerically has been studied. The results showed that by raising the Reynolds number, aspect ratio, volume fraction and amplitude the average Nusselt number will increase. Enhancement aspect ratio from 1 to 20, as a result of the simultaneous increase in the developing length, penetration of the jet flow in to the duct, and length of the recirculation zones, more than 12 percent enhancement in averaged Nusselt number on the lower wall is detected. Furthermore, it was showed in the investigations that increasing the Reynolds number, aspect ratio and amplitude the length of the recirculation zones rise.

This has a direct impact on the local Nusselt number which consequently increases the average Nusselt number. The present computations reveal that when the volume fraction increases gradually from 0.0 to 0.05 the averaged Nusselt numbers will be increase 14 percent. Also 24 percent enhancement in averaged Nusselt number is seen by increasing amplitude from 0.0 to 0.04. It should be noted the intensification of turbulence eddy transport, thinning of the boundary layer, dispersion of the suspended particles, and augmentation of thermal conductivity and heat capacity of the fluid were suggested to be the possible reasons for heat transfer enhancement.

REFERENCES

- [1] Choi S. U. S., (1995), Enhancing thermal conductivity of fluids with nanoparticles in developments and applications of non-Newtonian flows. *ASME FED* 231/ MD 66: 99–103.
- [2] Koblinski P. P., Choi S. U. S., Eastman J. A., (2002), Mechanisms of heat flow in suspensions of nano-sized particles (nanofluid). *Int. J. Heat. Mass. Trans.* 45: 855–863.
- [3] Eastman J. A., Phillpot S. R., Choi S. U. S., Koblinski P., (2004), Thermal transport in Nanofluids. *Annu. Rev. Mater. Res.* 34: 219–2 46.
- [4] Zhang Y., Li L., Ma H. B., Yang M., (2009), Effect of Brownian and Thermophoretic Diffusions of Nanoparticles on Nonequilibrium Heat Conduction in a Nanofluid Layer with Periodic Heat Flux. *Num. Heat. Transf. part A.* 56: 325 – 341.
- [5] Ravikanth S. V., Debendra K. D., Devdatta P. K., (2010), Development of new correlations for convective heat transfer and friction factor in turbulent regime for nanofluids. *Int. J. Heat. Mass. Trans.* 53: 4607-4618.
- [6] Sundar S. L., Sharma K.V., (2010), Turbulent heat transfer and friction factor of Al₂O₃ Nanofluid in circular tube with twisted tape inserts. *Int. J. Heat. Mass. Trans.* 53: 1409-1416.
- [7] Duangthongsuk W., Wongwises S., (2010), An experimental study on the heat transfer performance and pressure drop of TiO₂-water nanofluids flowing under a turbulent flow regime. *Int. J. Heat. Mass. Trans.* 53: 334-344.
- [8] Fotukiana S. M., Esfahany M. N., (2010), Experimental investigation of turbulent convective heat transfer of dilute -Al₂O₃/water nanofluid inside a circular tube. *Int. J. Heat. Fluid. Flow.* 31: 606-612.
- [9] Ghaffari O., Behzadmehr A., Ajam H., (2010), Turbulent mixed convection of a nanofluid in a horizontal curved tube using a two-phase approach. *Int. Communi. Heat. Mass Trans.* 37: 1555-1558.
- [10] Nishimura T., Matsune S., (1998), Vortices and wall shear stresses in asymmetric and symmetric channels with sinusoidal wavy walls for pulsatile flow at low Reynolds numbers. *Int. J. Heat. Fluid. Flow.* 19: 583-593.
- [11] Tolentino F. O., Mendez R. R., Palomares B. G., Guerrero A. H., (2009), Use of diverging or converging arrangement of plates for the control of chaotic mixing in symmetric sinusoidal plate channels. *Exp. Ther. Fluid. Scie.* 33: 208–214.
- [12] Habi M. A. B, Ikra U.H. M, Badr H. M., Said S. A. M., (1998), Calculation of Turbulent Flow and Heat Transfer in Periodically Converging-Diverging Channels. *Compute. Fluid.* 27: 95-120.
- [13] Pham M. V., Plourde F., Doan S. K., (2008), Turbulent heat and mass transfer in sinusoidal wavy channels. *Int. J. Heat. Fluid. Flow.* 29: 1240- 1257.
- [14] Zhang J., Muley A., Borghese J. B., Manglik R. M., (2003), Computational and experimental study of enhanced laminar flow heat transfer in three dimensional sinusoidal wavy-plate-fin channels, In: ASME Summer Heat Transfer Conference. *Las Vegas, NV, July* 21–23.
- [15] Yang X. D., Ma H. Y, Huang Y. N., (2005), Prediction of homogeneous shear flow and a backward-facing step flow with some linear and non-linear K–e turbulence models. *Communi. Nonlin. Scie. Nume. Simul.* 10: 315–328.
- [16] Driver D., Seegmiller H., (1985), Features of reattaching turbulent shear layer in divergent channel flow. *AIAA J.* 23: 163-171.
- [17] Shariati M., Bibeau R., Salcudean E., Gartshore M. I., (2000), Numerical and Experimental Models of Flow in the Converging Section Of A Headbox. *TAPPI Papermakers Conference, Vancouver, Canada.*
- [18] Xiaosi Z., (2001) Fiber orientation in Headbox, Msc thesis, University of British Columbia.
- [19] Feng X., Dong S., Gartshore I., Salcudean M., (2005), Numerical Model of Fiber Orientation in the Converging Section of a Paper-machine Headbox using Large Eddy Simulation, Fourth International Conference on CFD in the Oil and Gas, *Metallurgical & Process Industries SINTEF / NTNU Trondheim.* Norway.
- [20] Sarma A. S. R., Sundararajan T., Ramjee V., (2000), Numerical simulation of confined laminar jet flows. *Int. J. Nume. Meth. Fluid.* 33: 609–626.
- [21] Battaglia F., Tavener S. J., Kulkarni A. K., Merkle C. L., (1997), Bifurcation of low Reynolds number flows in symmetric channels. *AIAA J.* 35: 99–105.
- [22] Al-Aswadi A. A., Mohammed H. A., Shuaib N. H., Campo A., (2010), Laminar forced convection flow over a backward facing step using nanofluids. *Int. Commu. Heat. Mass. Trans.* 37: 950–957.

- [23] Launder B. E., Spalding D. B., (1972), Lectures in Mathematical Models of Turbulence. *Academic Press*. London.
- [24] Rostamani M., Hosseinizadeh S. F., Gorji M., Khodadadi J. M., (2010), Numerical study of turbulent forced convection flow of nanofluids in a long horizontal duct considering variable properties. *Int. Commun. Heat. Mass. Trans.* 37: 1426-1431.
- [25] Chon C. H., Kihm K. D., Lee S. P., Choi S. U. S., (2005), Empirical correlation finding the role of temperature and particle size for nanofluid (Al_2O_3), Thermal conductivity enhancement. *Appl. Phys. Lett.* 87: 153107–153110.
- [26] Mintsu H. A., Roy G., Nguyen C. T., Doucet D., (2009), New temperature dependent thermal conductivity data for water-based Nanofluids. *Int. J. Ther. Scie.* 48: 363–371.
- [27] Masoumi N., Sohrabi N., Behzadmehr A. A., (2009), New model for calculating the effective viscosity of nanofluids. *J. Phys D: Appl. Phys.* 42: 55501-55506.
- [28] Pak B. C., Cho Y. I., (1998), Hydrodynamic and heat transfer study of dispersed fluids with submicron metallic oxide particles. *Expe. Heat. Trans.* 11: 151–170.

How to cite this article: (Vancouver style)

Taheri A., Aboukazempour E., Ramiar A., Ranjbar A. A., Rahimi-Esbo M., (2016), Numerical study of turbulent forced convection nanofluid jet flow in a converging sinusoidal channe. *Int. J. Nano Dimens.* 7(1): 57-70.

DOI: [10.7508/ijnd.2016.01.007](https://doi.org/10.7508/ijnd.2016.01.007)

URL: http://ijnd.ir/article_15585_2444.html